Polymer Chemistry

PAPER

Cite this: *Polym. Chem.*, 2015, **6**, 7036

Synthesis of random terpolymers bearing multidentate imidazole units and their use in functionalization of cadmium sulfide nanowires

Anand Viswanath, Pravin Paudel, Preecha Kittikhunnatham, Alexandra N. Green, Andrew B. Greytak and Brian C. Benicewicz*

Received 9th May 2015,
Accepted 14th August 2015

DOI: 10.1039/c5py00685f

www.rsc.org/polymers

This work reports on a new random ternary polymerization method for the synthesis of multidentate imidazole polymers. The polymers can behave as ligands for the functionalization of cadmium sulfide nanowires. Due to the intrinsic differences in the electronegativity of the groups next to the vinyl bond, the vinyl groups displayed unique NMR signals, and allowed for the measurement of the individual monomer conversions in the random terpolymer system. The activated ester bearing terpolymer was postmodified with *N*-alkyl imidazole units, followed by the boc deprotection of the amine terminal groups. The resulting poly(imid-PEGMA-MAMamine) provided water solubility, dye loading capability as well as the ability to coordinate with metal chalcogenide surfaces using the imidazole units. Upon the attachment of a rhodamine dye, studies were performed to analyze the potential of such polymers to modify CdS nanowires using fluorescence microscopy. The fluorescence microscopy results provided confirmation of the polymeric ligand attachment, and sets the foundation for further optical studies using this system.

Introduction

Semiconductor nanowires have been extensively studied as a potential candidate for various electronic devices like photovoltaics, transistors and photodetectors because of their unique size and structure dependent optical and electronic properties.[1–3] Since these materials have high surface to volume ratios, the surface structure of nanowires (NWs) plays an important role in the performance of these electronic devices.[4] For the case of cadmium sulfide (CdS), a representative compound semiconductor with a direct bandgap in the visible spectrum, various groups have explored the properties of cadmium sulfide (CdS) nanomaterials by tailoring their shape (nanosheets, platelets)[5,6] and through the use of ligands[7–9] that can coordinate to the nanomaterial surface. The use of ligands to tune the optical and electronic properties of nanoscale semiconductors is particularly appealing as it potentially allows a one-step functionalization or ligand exchange with a wide choice of ligand structures to enable control of low temperature assembly, biological interfaces, and patterning independently of crystal growth steps.

A variety of small molecule ligands have been used in the literature to coordinate to CdS surfaces, including phosphates,[10] thiols[11] and carboxylic acids.[12] Recently, polymeric materials containing these functional groups have been utilized to not only tune the properties of the CdS surface, but also to build robust functionalization, for example to promote the dispersion of nanocrystals into polymer matrices.[11,13] Polymeric imidazoles have shown promise in recent reports as an efficient binder to colloidal nanocrystals (quantum dots) composed of CdS and related chalcogenides.[14–20] For the attachment of small molecules or polymer brushes to CdS surfaces in the absence of a matrix or observable changes in solubility, two challenges are prominent: choice of the appropriate ligand functionality and effective characterization of the functionalized CdS surface to establish that the coating is anchored to the substrate. Binding of imidazoles to CdS and similar surfaces is believed to be driven by a metal affinity interaction between imidazole nitrogen and surface cadmium atoms.[21] Proteins and synthetic polymers with multiple imidazole groups exhibit strong binding and have been described as multi dentate,[14] though structural and thermodynamic details remain sparse. We sought to determine whether polymeric imidazole ligands could be used to functionalize the native surface of vapor-deposited CdS NWs. The development of deliberate polymer strategies to functionalize CdS NWs has not been reported, nor are we aware of previous examples in which fluorescently-labeled ligands have been employed to directly probe ligand binding to compound semiconductor NWs.

In this work, using the RAFT polymerization technique, imidazole monomers were copolymerized with polyethylene glycol methacrylate and boc-protected methacrylate to add

Department of Chemistry and Biochemistry, University of South Carolina, Columbia, South Carolina 29208, USA. E-mail: benice@sc.edu

This journal is © The Royal Society of Chemistry 2015

water solubility and dye attachment capabilities to the polymer. The RAFT method also afforded polymers that can be intricately tailored, possessed low polydispersities, and contained active sites for subsequent modification. Furthermore, the unique choices of monomer structures enabled the use of a simple NMR technique to investigate kinetics and compositions, which can be useful for other studies with multiple monomers. More importantly, the protocols developed herein for functionalized CdS NWs were scalable in conjunction with simplified processes for commercial viability.

The ternary copolymer (terpolymer) allows three different functions to be incorporated including multiple imidazoles for binding/attachment to the CdS surface, PEG chains for solubility in aqueous media, and primary amines for attachment of a payload: here, a fluorescent dye. We demonstrate the utility of a methacrylate-based terpolymer by testing whether the imidazole binding motif used to prepare water-soluble nanocrystals (NCs) *via* ligand exchange can also spontaneously associate to chalcogenide NW surfaces prepared by physical vapor deposition. Essentially, a successful binding of terpolymer ligand on the nanowire surface has been shown. It has also been shown that fluorescence microscopy can be a good technique to illustrate ligand binding on nanowire surfaces using a dye. This has been accomplished by labeling the terpolymer with a rhodamine dye, and binding the terpolymer on CdS nanowire surface using imidazole units in the terpolymer.

Experimental

Materials and methods

All reagents were used as received from Fisher Scientific unless stated otherwise below. AIBN was purchased from Sigma Aldrich and recrystallized thrice from methanol. Poly(ethyleneglycol) methacrylate (500 g mol^{-1}) was obtained from Sigma Aldrich and passed through a neutral alumina column to remove inhibitors before use. 4-Cyano-4 [(dodecylsulfanylthiocarbonyl)sulfanyl]pentanoic acid (CDTPA) was obtained from Strem Chemicals, Inc. NMS (*N*-methacryloxy succinimide) was synthesized from NHS (*N*-hydroxy succinimide) as described in the literature.[22] *tert*-Butyl (2-(2-(2-methacrylamidoethoxy)-ethoxy)ethyl)carbamate (MAMboc) was synthesized according to a similar procedure as outlined by Liu and coworkers.[15]

Characterization

NMR spectra were recorded on a Varian Mercury 300 spectrometer using $CDCl_3$ or D_2O as the solvent. The molecular weights and molecular weight distributions were determined using a Waters gel-permeation chromatograph equipped with a 515 HPLC pump, a 2410 refractive index detector, three Styragel columns (HR1, HR3, HR4 in the effective molecular weight range of 100–5000, 500–30 000, and 5000–500 000, respectively). Tetrahydrofuran (THF) was used as the eluent at 30 °C and a flow rate of 1.0 mL min^{-1}. The GPC system was calibrated with polystyrene standards obtained from Polymer Laboratories. FT-IR spectra were recorded on a Perkin Elmer Spectrum 100 using an attenuated total reflection diamond cell attachment. Confirmation of binding of polymer dye ligand on NW surface was performed using fluorescence microscopy. Dark field scattered light and corresponding fluorescence images were recorded. The emission peak of the NWs is at *ca.* 505 nm, and the dye emission peak is at 590 nm. The fluorescence microscopy setup has an excitation wavelength longer than that of the NWs in order to avoid NW excitation. Emitted light was passed through a 590 nm long pass filter to select fluorescence from the dye only. Images were collected through a 20× objective lens with numerical aperture 0.45.

Preparation of poly(NMS-PEGMA-MAMboc)

In a typical copolymerization, 4-cyano-4-(dodecylsulfanylthiocarbonyl)sulfanylpentanoic acid (CDTPA) (0.01 g, 0.0123 mmol), NMS (0.0675 g, 0.369 mmol), PEGMA (500 g mol^{-1}, 0.185 g, 0.369 mmol), MAMboc (0.117 g, 0.369 mmol), trioxane (internal standard) (18.4 mg), and AIBN (0.00246 mmol, 0.004 g) were dissolved in 1.35 mL of THF. The mixture was stirred until all the reactants were dissolved, placed in a Schlenk tube and subjected to three cycles of freeze–pump–thaw. The tube was then heated at an oil bath temperature of 65 °C for 20 h. The polymerization was quenched in ice water and the mixture precipitated in diethyl ether. The mixture was centrifuged at 3000 rpm for 5 min and redispersed in 3 mL of THF. This precipitation-redispersion process was repeated twice to obtain poly (NMS-PEGMA-MAMboc) with M_n: 19 865, PDI: 1.29.

Preparation of poly(imid-PEGMA-MAMboc)

The poly(NMS-PEGMA-MAMboc) (0.5 g, 0.369 mmol of NMS content) was dissolved in 10 mL THF in a 50 mL two neck RB flask, followed by the addition of 3-aminopropyl imidazole (0.046 g, 0.372 mmol) and triethylamine (0.056 g, 0.558 mmol) at room temperature. The mixture was sparged with N_2 for 15 min, and then heated at 70 °C overnight. The reaction was cooled and the polymer was precipitated in diethyl ether (30 mL). The mixture was then centrifuged at 3000 rpm for 5 min to separate out the unreacted imidazole, and the polymer redispersed in THF (10 mL). The precipitation–centrifugation–redispersion process was repeated twice more to ensure complete removal of the free imidazole and obtain the purified poly(imid-PEGMA-MAMboc) (0.48 g).

Preparation of poly(imid-PEGMA-MAMamine)

Poly(imid-PEGMA-MAMboc) (0.275 g, 0.25 mmol of boc content) was dissolved in DCM (3 mL) and cooled to 0 °C. Trifloroacetic acid (TFAA) (2 mL) was added dropwise to the stirring mixture. The mixture was allowed to warm to room temperature and stirred for 12 h. The mixture was precipitated in ether to recover the boc deprotected polymer, and the solvent was removed under vacuum. The polymer was dissolved in methanol (5 mL) and a solution of NaOH in methanol was added dropwise until the pH of the solution adjusted to 7–9. The methanol was evaporated to yield a white solid of

poly(imid-PEGMA-MAMamine) (0.2 g). Using ^{1}H-NMR analysis of the boc methyl protons of the starting material at 1.43 ppm, 100% deprotection of the boc group was observed.

Conjugation of amine functional terpolymer with rhodamine dye

Commercially available 5-(and-6)-carboxy-X-rhodamine succinimidyl ester (5(6)-ROX, SE) was dissolved in dry DMSO to make a stock solution of dye. A known amount of amine functional polymer was dissolved in aqueous 0.1 M $NaHCO_3$ solution. 10 equivalents of dye (per polymer chain) were mixed with polymer solution and were continuously vortexed for 2 hours to achieve polymer–dye conjugation. Excess dye was removed by dialysis with bicarbonate buffer using 10 K MW cutoff centrifugal filters; centrifugal dialysis was continued until eluent was clear. The total concentration of dye in the final product was calculated using UV-visible absorption spectroscopy. Assuming no polymer was lost during dialysis and transferring, the average number of dyes per polymer chain was calculated to be 0.25; this number therefore represents a lower bound.

CdS nanowire growth

CdS nanowires were grown by physical vapor transport of CdS powder in presence of 40 nm gold colloids supported on Si wafer substrates to promote VLS growth of NWs in Ar atmosphere using a modification of previously described procedures.[23] The morphology of CdS nanowires was studied using scanning electron microscopy (SEM). The growth substrate has both nanowires (40–200 nm in diameter), and nanobelts (1–4 μm diameter) that range from a few micrometers to tens of micrometers long.

Treatment of nanowires with polymer dye conjugate solution

CdS NWs on the growth substrate were treated with dye-labeled polymer solution (total dye concentration: 5 μM) for 2 hours. After 2 hours, the substrate was thoroughly rinsed with aqueous $NaHCO_3$ solution. As a control, a similar substrate with CdS NWs was treated with 5 μM free dye solution for 2 hours and similarly rinsed. NWs were then dispersed in aqueous solution by sonication; a drop of this suspension was placed on a glass slide, covered with a glass cover slip, and observed through the microscope.

Results and discussion

RAFT polymerization of poly(NMS-PEGMA-MAMboc)

In this strategy, an activated succinimide ester was directly copolymerized along with PEGMA and the MAMboc monomer (Scheme 1). Several reports have investigated the use of an imidazole bearing monomer, but this has disadvantages including degradation of the RAFT agent by the nucleophilic imidazole and limited solubility parameters of the polymer (especially for analysis by GPC).[24] Accordingly, the NMS monomer allows for postmodification to obtain the imidazole group, enables solubility in many common organic solvents, and maintains the integrity of the RAFT agent. The boc protected monomer (MAMboc) enables the polymerization of a protected amine monomer. Again, using a simple postmodification, the amine can be accessed for attachment to dyes. PEGMA (500 g mol^{-1}) was chosen to supply water soluble characteristics to the terpolymer, as the coordination of the polymer with the CdS NWs was performed in aqueous media.

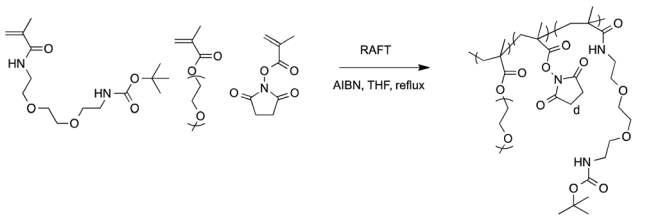

Scheme 1 Preparation of terpolymers of NMS, PEGMA and MAMboc using RAFT polymerization.

Additionally, the monomer functionalities present in the copolymerization mixture include a methacrylate (PEGMA), a methacrylamide (MAMboc) and a methacrylate derivative (NMS). Due to the difference in electronegativities of the functional groups next to the vinyl bonds in the monomers, the vinyl terminal CH_2 signals are discrete for each monomer in the ^{1}H-NMR spectrum (Fig. 1). Typically, comonomer mixtures have overlapping vinyl signals, which makes the analysis of individual monomer conversions difficult. In many cases, block copolymerization has been attempted as an alternative approach to calculate monomer conversions.[25] However, through a random copolymerization strategy, the individual monomer conversions and composition in the copolymer can be analyzed in detail in this polymerization system *via* measuring the integrations of the monomer signals compared to that of 1,3,5-trioxane. As seen in Fig. 2, the decrease in monomer signal intensity is seen as the polymerization progresses at reflux when 0.15 eq. of AIBN is used. The kinetics of the polymerization can then be analyzed by removing a small sample under nitrogen for analysis by ^{1}H-NMR. This approach is unique as such a method for kinetic analysis has not been reported previously for a random terpolymerization method,

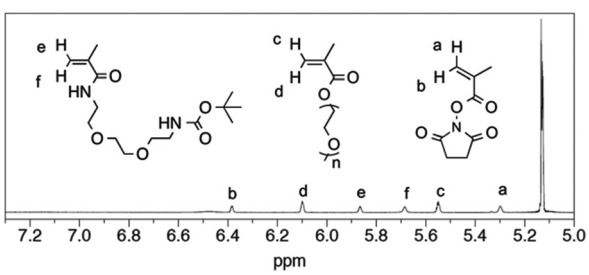

Fig. 1 ^{1}H-NMR spectrum of the polymerization mixture in $CDCl_3$ showing the discrete monomer signals. An equimolar ratio (50 : 50 : 50 : 1 of NMS : PEGMA : MAMboc : RAFT) is used, along with 0.15 eq. of AIBN. Trioxane (5.13 ppm) is also present as an internal standard.

This journal is © The Royal Society of Chemistry 2015

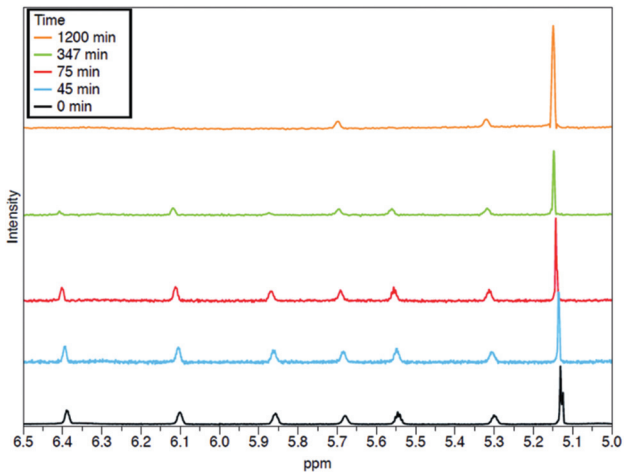

Fig. 2 ^{1}H-NMR spectra of the polymerization mixture in $CDCl_3$ at various polymerization times showing an inverse relationship between monomer signal intensity and polymerization.

mainly due to complications in the vinyl signal overlap in the various monomers.

The overall kinetics of the random copolymerization revealed a linear relationship of molecular weight (M_n) with the total monomer conversion, suggesting the controlled growth of polymer chains in the polymerization (Fig. 3, top). The M_n as obtained from GPC deviated at varying points from the theoretical M_n, and is likely due to the inaccuracy of the GPC (polystyrene calibration) with respect to M_n for this particular multifunctional polymer. The polymers at various conversions also displayed low polydispersities and a gradual decrease in polydispersity over the total monomer conversion, and this points to the control afforded by the RAFT polymerization technique. Further evidence is also provided by Fig. 3 (bottom), where a linear relationship between $\ln([M_o]/[M_t])$ and time is displayed. $[M_o]$ is the initial total monomer concentration and $[M_t]$ is the final total monomer concentration at various times in the polymerization. This supports the theory of control in RAFT where the concentration of the growing species remains constant and first-order kinetics is achieved.

Although the kinetic curves provided an overview of the total monomer consumption with time, there was a need to study the individual monomer conversions to investigate the exact composition of the polymer at various reaction times. This can be important in cases where the composition of the polymer can affect performance: for example, lower amounts

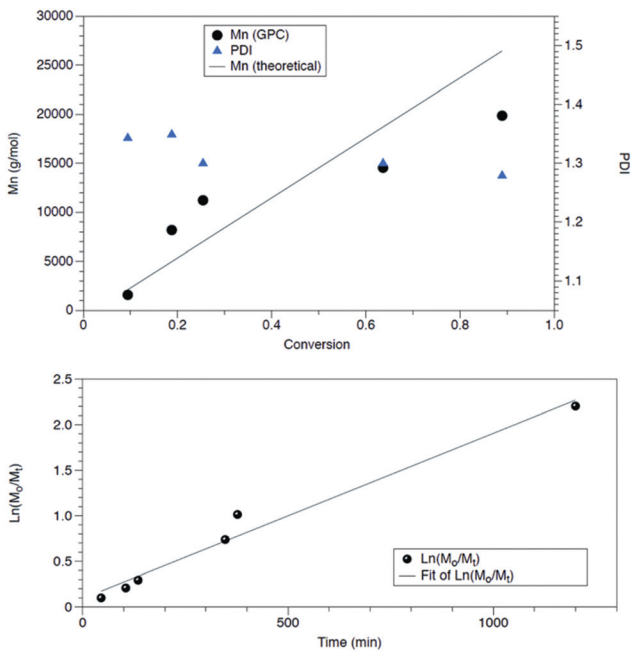

Fig. 3 Kinetic curves for the RAFT polymerization of NMS, PEGMA and MAMboc with a monomer ratio of 50 : 50 : 50 using chain transfer agent CDTPA and AIBN with a ratio of 1 : 0.15 in DMF at 80 °C. (Top) evolution of M_n and PDI with total monomer conversion and (Bottom) semilogarithmic plot *versus* time.

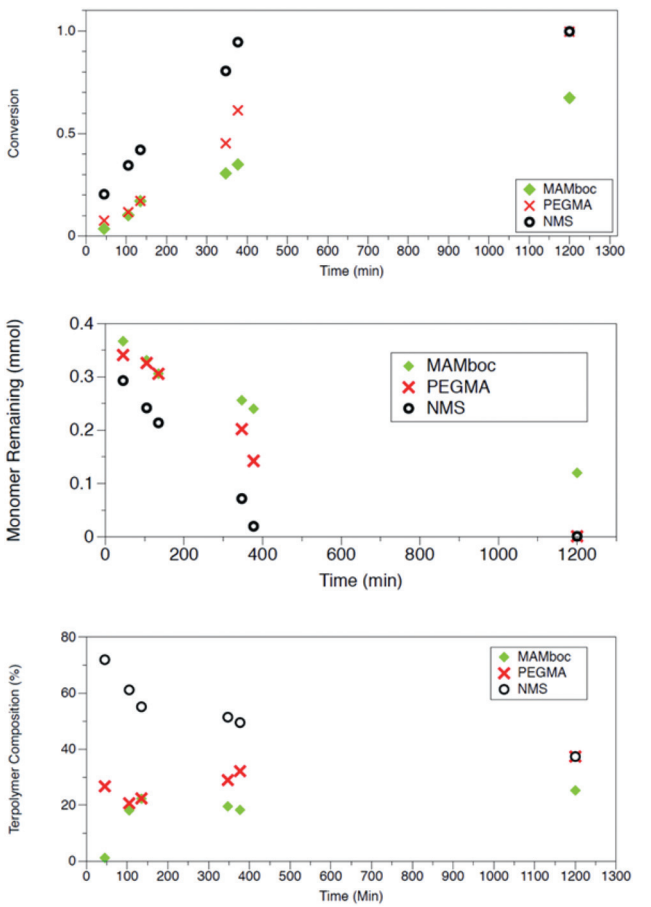

Fig. 4 (Top) Individual monomer conversions at different reaction times in the RAFT copolymerization of NMS, PEGMA and MAMboc with a ratio of 50 : 50 : 50 in the presence of CDTPA and AIBN (1 : 0.15 eq.). (Middle) The monomer remaining in the copolymerization mixture with varying reaction time. (Bottom) Total terpolymer composition at different reaction times.

Table 1 Table showing individual monomer conversions, M_n and PDI results at varying times in the copolymerization of NMS, PEGMA and MAMboc (50 : 50 : 50) with using CDTPA and AIBN (1 : 0.15 eq.) at reflux in THF

Time (min)	MAM conv. (%)	PEG conv. (%)	NMS conv. (%)	Total conv. (%)	Theo M_n (g mol^{-1})	M_n (GPC) (g mol^{-1})	PDI
45	2.75	2.31	4.32	3.1	965	4030	1.23
67	10.5	16.31	54	26.9	4675	9898	1.31
85.5	27.34	32.54	61.41	40.4	7630	11 307	1.3
257	45.33	64.39	99.47	69.7	13 350	19 880	1.3

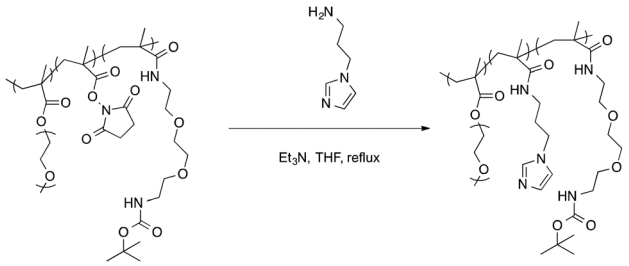

Scheme 2 Preparation of poly(imid-PEGMA-MAMboc) using 3-amino propyl imidazole.

of the PEG content can inhibit water solubility characteristics. As seen in Fig. 4 and Table 1, the NMS monomer displayed an increased propensity to be consumed during the polymerization as compared to the other monomers. This behavior was also observed in other copolymerizations, including with butyl acrylate[26] and *N*-(2-hydroxypropyl) methacrylamide (HPMA).[27] As seen in Fig. 4, the trend for the reactivity of monomers is NMS > PEGMA > MAM-boc. It is interesting that MAMboc is not fully consumed in the polymerization, while the other two monomers are able to achieve 100% conversion. Another interesting aspect is that NMS and PEGMA both tend to react faster than the MAMboc, and this observation correlates well with other studies in the literature, where NMS and methacrylate based polymers tend to have higher reactivity ratios than the corresponding methacrylamides.[28–30] The relationship between NMS and methacrylates has not been extensively reported in the literature, but work on their dual copolymerization revealed a higher reactivity ratio for NMS compared to PEGMA.[31] Thus, the reactivity trends seen in Fig. 4 can be understood by analyzing the fundamental reactivity relationships of the different monomer pairs.

Ideally, reactivity ratio studies can be performed for dual monomer systems using established methods such as the Kelen-Tudos or Fineman-Ross, but terpolymer reactivity ratio calculations require the use of ternary plots and are limited in the literature.[32] A viable alternative to obtain a quick understanding of the relative reactivities is provided through these studies. Essentially, the growing chain is richer in NMS units initially, and due to the drastic decrease in concentration of NMS as the polymerization progresses, the polymers chains start to incorporate additional PEGMA units, leaving the tail end of the polymer heavily composed with MAM-boc units (Fig. 4). The trend in reactivity observed with these monomers confirms the presence of a pseudo gradient polymer. The randomization of monomer units also avoids complications related to the solubility if prepared by a block copolymerization method. It was observed that NMS homopolymers tended to precipitate out of the solvent, and a large amount of PEGMA units was needed for water solubility.

Synthesis of poly(imid-PEGMA-MAMboc)

Using a simple postmodification strategy of cleaving succinimide with amines, the poly(NMS-PEGMA-MAMboc) was dissolved in THF, followed by the addition of triethylamine (catalyst) and the imidazole (Scheme 2). After the reaction, the polymer was precipitated with diethyl ether, followed by centrifugation to purify the polymer. Typically, the imidazole used for such polymers involve hydrochloride salts, for *e.g.* histamine salts. Ionic imidazoles are often incompatible for reactions in organic media, and when polymeric reactions are done in water, the product has to undergo a time-consuming dialysis process in water, followed by an expensive lyophilization step (to remove the water while preserving the polymer functionality) to facilitate the removal of the excess imidazole reactant. Furthermore, the imidazole used herein (3-amino propyl imidazole) has shown to be useful as a coordinating ligand in quantum dots,[16] and is significantly less expensive than other commercially available imidazole based amine linkers. The reaction of the succinimide with amines is known to be a highly efficient reaction, with high yields under mild reaction conditions.[33] The characterization of this reaction is further discussed in later sections.

Synthesis of poly(imid-PEGMA-MAMamine)

The boc deprotection of polymers typically involves a reaction with conc. HCl solution. However, the boc deprotection of poly(imid-PEGMA-MAMboc) was not successful with various HCl solutions (0.3–1 M) and increased temperatures (20–40 °C). However, trifloroacetic acid (TFAA) proved to be an efficient deprotection agent (Scheme 3), where the boc peak at 1.43 ppm in the ^{1}H-NMR was completely removed (see Fig. 5). In this reaction, the TFAA protonates *tert*-butyl carbamate followed by decarboxylation and releases the amine product. The polymer undergoes precipitation in ether to remove any starting material, and excess TFAA is removed under vacuum. The pH of the polymer is adjusted to 7–8 to neutralize any residual acid in the mixture.

NMR and IR characterization of the terpolymers

The reaction of poly(NMS-PEGMA-MAMboc) with the imidazole was monitored by ^{1}H-NMR, where the product displayed characteristic peaks from the imidazole from 6.8 ppm to 6.95 ppm and at 7.35 ppm (Fig. 5). The succinimide peaks of the starting material (expected to be a broad peak at 2.75–2.85 ppm) were overshadowed by the CH_2 next to the imi-

 This journal is © The Royal Society of Chemistry 2015

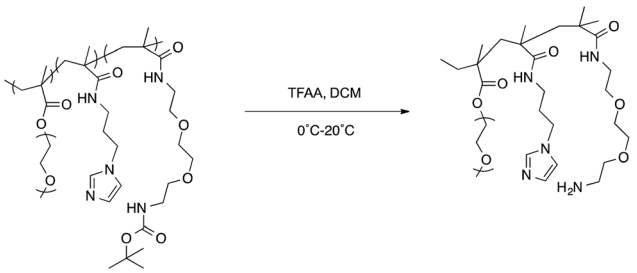

Scheme 3 Boc deprotection of poly(imid-PEGMA-MAMboc) with TFAA.

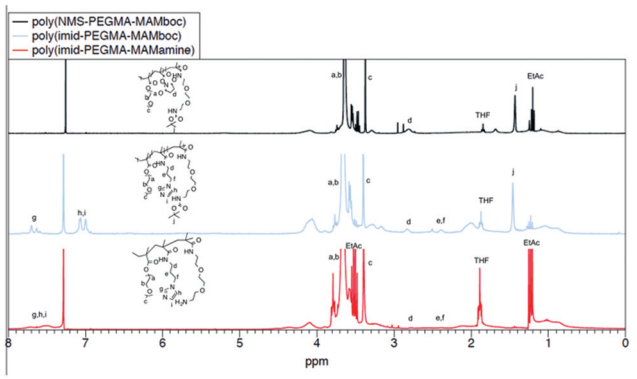

Fig. 5 ^{1}H-NMR spectrum of poly(NMS-PEGMA-MAMboc), poly(imid-PEGMA-MAMboc) and poly(imid-PEGMA-MAMamine) in $CDCl_3$.

dazole unit, and was difficult to calculate the conversion of the imidazole in this manner. The PEGMA peaks (3.7–3.85 ppm) and the boc methyl peaks (1.43 ppm) from the MAMboc units were retained without degradation in the product, which illustrated the relatively mild conditions used for the imidazole attachment reaction. The replacement of the succinimide units by the imidazole was also confirmed through IR analysis, where the C═O in the succinimide clearly showed a significant decrease in intensity at 1700 cm^{-1} (Fig. 6). The presence of the imidazole units could not be confirmed by IR, as the imidazole signals (at 1130 and 1484 cm^{-1}) were obscured by broader peaks corresponding to the C–N stretches from the succinimide in the poly(NMS-PEGMA-MAMboc). For the removal of the boc group in poly(imid-PEGMA-MAMboc), the boc peak at 1.43 ppm was monitored with ^{1}H-NMR, and the complete disappearance of the boc peak was observed after the reaction with TFAA. The terminal amine signal could not be confirmed with ^{1}H-NMR, and was confirmed *via* a ninhydrin stain method, where a purple stain was obtained (the starting material poly(imid-PEGMA-MAMboc) gave a pale yellow stain in the ninhydrin test). It must be noted that a shift in the imidazole signals was also seen, with the CH peaks on the imidazole ring broadening at 7.1–8 ppm, and may be the result of the imidazole amine coordinating with the TFAA salts.

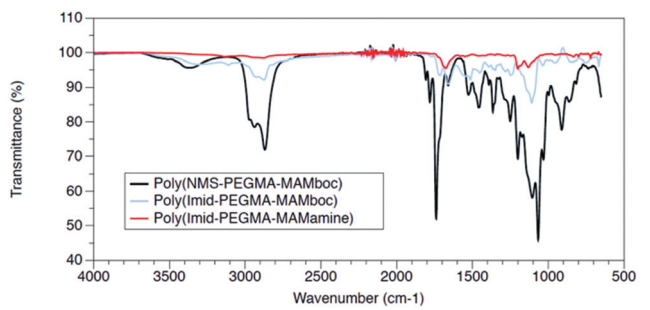

Fig. 6 IR spectra showing the changes in functionality at various points in the synthetic route.

Dye labeled polymer binding on NW surfaces

We selected CdS nanowires synthesized by a physical vapor transport method. The growth substrate was examined with field-emission scanning electron microscopy and was found to contain primarily NWs (40–200 nm in diameter) as well as some nanobelts with widths up to a micron (Fig. 7). UV-visible absorption spectroscopy of the free dye and dye labeled polymer revealed little change in the peak position or lineshape (Fig. 8). Based on the absorbance of the purified polymer–dye sample measured at a known dilution, and the published extinction coefficient of the ROX dye, we determined an average dye–per-polymer ratio of 0.25. In order to confirm the attachment of the dye-functionalized polymer to the NW substrate, fluorescence microscopy was used to analyze the CdS NWs treated with the dye functionalized polymer and with the free rhodamine dye. Dark field microscopy was used to locate single nanowires, while the fluorescence image, which is sensitive only to dye emission, is used to identify localization of the dye to the NW surface.

Fig. 9 shows representative darkfield and fluorescence images of a NW treated with the dye labeled terpolymer. The NW is clearly visible in darkfield mode owing to high dielectric

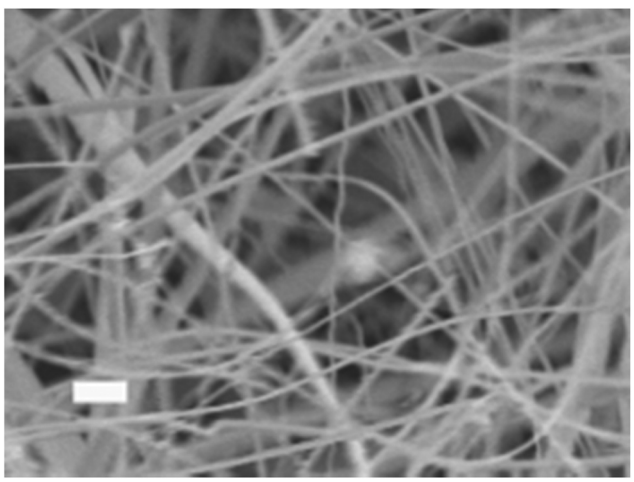

Fig. 7 SEM image of CdS nanowire sample supported on Si growth substrate. Scalebar, 1 μm.

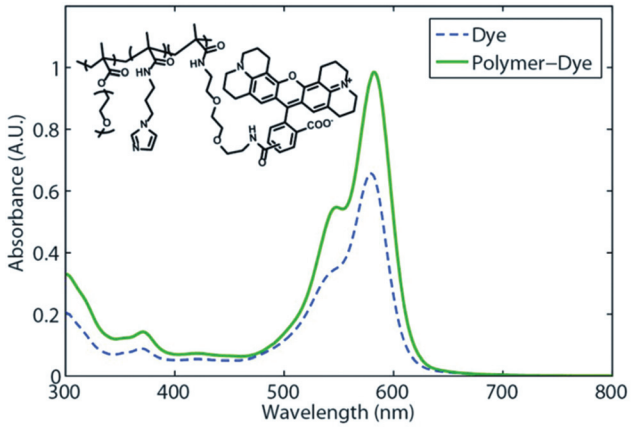

Fig. 8 UV-visible absorption spectra of dye-labeled polymer (solid line) and free dye reference (dashed line) in 0.1 M $NaHCO_3$.

contrast with the surrounding medium. The NW is also clearly visible in fluorescence mode when illuminated with sub-bandgap light at the dye excitation wavelength. The prominent fluorescence signal demonstrates clearly the presence of the dye labeled polymer on the NW surface. Fig. 10 shows a representative images from the control experiment in which NWs were exposed to a solution of the free dye. In the fluorescence image, at the location of the NW, the signal cannot be distinguished from background.

A particular advantage of NWs as a target for fluorescence measurement of ligand binding to inorganic surfaces is their quasi one-dimensional shape; the fluorescence intensity profile measured orthogonal to the NW should vary slowly with respect to translation along the NW axis. The dark field and fluorescence intensity traces shown in Fig. 9 and 10 represent profiles averaged along the NW axis over a width represented by the red boxes in the images; this analysis improves the signal to noise ratio and helps in distinguishing the NW intensity signal from background. The absence of a fluo-

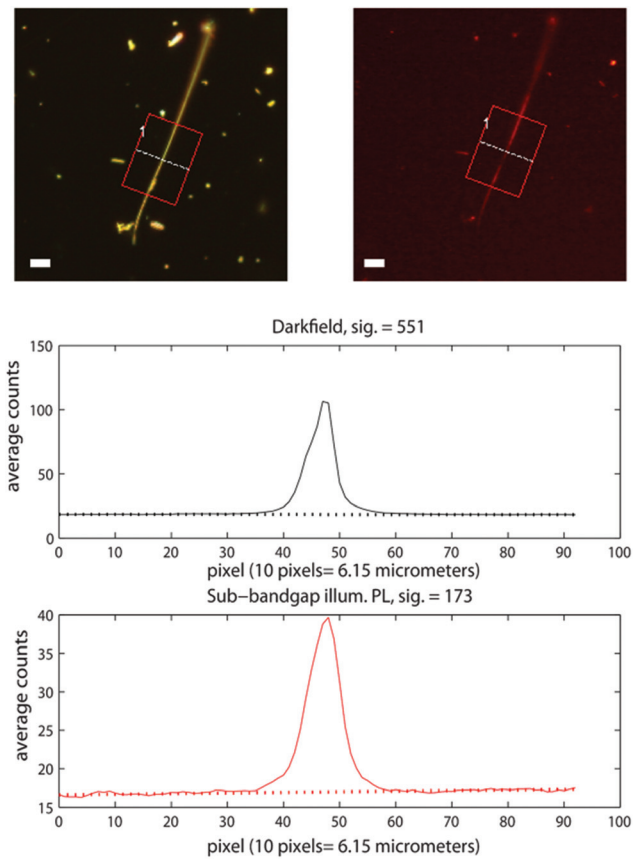

Fig. 9 Optical micrographs of a representative CdS NW treated with dye-labeled terpolymer ligand. (Top left) True color image of NW in dark field mode. (Top right) False color image of the same location in fluorescence mode. Scale bars 10 μm. Dark field and fluorescence intensity profiles centered on the dashed lines marked "1" in the images are shown below. Traces represent the average of parallel profiles occupying the region indicated by the red boxes. The dashed lines represent the background intensity level as determined by a linear fit to data points at the extreme ends of the profile.

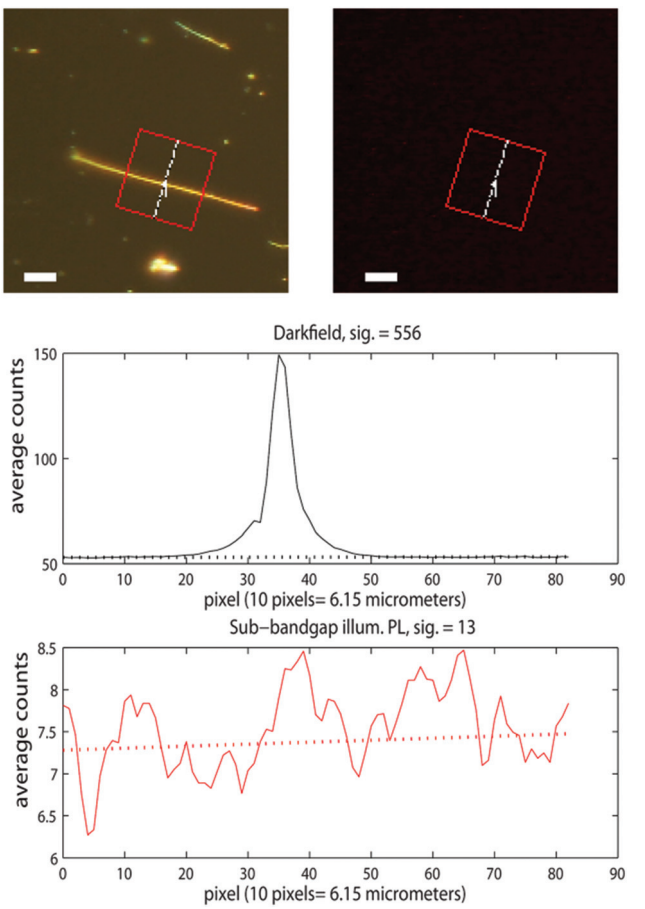

Fig. 10 Optical micrographs of a representative CdS NW treated with free carboxyrhodamine dye. (Top left) True color image of NW in dark field mode. (Top right) False color image of the same location in fluorescence mode. Scale bars 10 μm. Dark field and fluorescence intensity profiles centered on the dashed lines marked "1" in the images are shown below; note the vertical scale of the fluorescence trace is much smaller than shown in Fig. 9.

This journal is © The Royal Society of Chemistry 2015

rescence signal from the dye in the control case suggests that the free dye is incapable of complexing with the NW surface under the experimental conditions.

Comparison of the dye-labeled polymer treatment and the control experiment clearly identifies the ability of the terpolymer ligand units to simultaneously bind to the NW surface and the dye payload. These experiments confirm the hypothesis that a terpolymer with three discrete functionalities is capable of binding to unmodified CdS nanowire surfaces, and paves the path for new opportunities in the optoelectronic field.

Conclusion

A synthetic route for the preparation of random copolymers bearing imidazole, PEG and amine groups on a methacrylate backbone was developed. A dye-labeled version of this terpolymer has enabled confirmation of the functionalization of CdS NWs *via* single-NW fluorescence microscopy. The versatile route of using activated esters in copolymerization was shown to incorporate unique methods of measuring copolymer composition and synthesizing a pseudo-gradient copolymer. The kinetics of the polymerization were analyzed to reveal differences in reactivities of the monomers, which play a large role in copolymer composition. Additionally, the postmodification of the succinimide groups on the terpolymer with an organic imidazole proved to be a simple and scalable synthetic method. In the final step, cleavage of the boc groups provided amines capable of attaching to rhodamine dyes. The hypothesis that methacrylate-based polymeric imidazole ligands could coordinate to the native surface of CdS NWs grown by catalyzed vapor deposition has been confirmed. The development of polymers with a high degree of control and functionality may open up new opportunities in optoelectronic applications, and lead to a better understanding of the kinetics of binding various ligand structures to nanowire substrates. This could be valuable for applications of nanowires in optoelectronic devices and sensors, and for fundamental studies of the interactions of multidentate polymer ligands with the surfaces of technologically relevant compound semiconductor surfaces. We anticipate that similar methacrylate-based terpolymer ligands can be used for surface modification of a wide variety of colloidal and surface-bound inorganic nanomaterials.

Acknowledgements

This work was supported in part by the University of South Carolina through an Aspire grant to Andrew B. Greytak. We would like to acknowledge Christopher S. Pinion, Benjamin Gilbert, and Aaron Cameron for helpful discussions.

References

1 A. I. Hochbaum and P. Yang, *Chem. Rev.*, 2010, **110**, 527.
2 M. Law, J. Goldberger and P. Yang, *Annu. Rev. Mater. Res.*, 2004, **34**, 83.
3 C. M. Lieber and Z. L. Wang, *MRS Bull.*, 2011, **32**, 99.
4 Q. Hang, F. Wang, P. D. Carpenter, D. Zemlyanov, D. Zakharov, E. A. Stach, W. E. Buhro and D. B. Janes, *Nano Lett.*, 2008, **8**, 49.
5 T. Gao and T. Wang, *Cryst. Growth Des.*, 2010, **10**, 4995.
6 A. Prudnikau, A. Chuvilin and M. Artemyev, *J. Am. Chem. Soc.*, 2013, **135**, 14476.
7 Z. Ning, M. Molnár, Y. Chen, P. Friberg, L. Gan, H. Ågren and Y. Fu, *Phys. Chem. Chem. Phys.*, 2011, **13**, 5848.
8 A. Widmer-Cooper and P. Geissler, *Nano Lett.*, 2014, **14**, 57.
9 V. Rajendran, M. Lehnig and C. M. Niemeyer, *J. Mater. Chem.*, 2009, **19**, 6348.
10 N. Ma, E. H. Sargent and S. O. Kelley, *Nat. Nanotechnol.*, 2009, **4**, 121.
11 S. Chen, J. Zhu, Y. Shen, C. Hu and L. Chen, *Langmuir*, 2007, **23**, 850.
12 X. Li, V. M. Nichols, D. Zhou, C. Lim, G. S. H. Pau, C. J. Bardeen and M. L. Tang, *Nano Lett.*, 2014, **14**, 3382.
13 W. Jang, P. Koo, K. Bryson, S. Narayanan, A. Sandy, T. P. Russell and S. G. Mochrie, *Macromolecules*, 2014, **47**, 6483.
14 P. Zhang, S. Liu, D. Gao, D. Hu, P. Gong, Z. Sheng, J. Deng, Y. Ma and L. Cai, *J. Am. Chem. Soc.*, 2012, **134**, 8388.
15 W. Liu, A. B. Greytak, J. Lee, C. R. Wong, J. Park, L. F. Marshall, W. Jiang, P. N. Curtin, A. Y. Ting, D. G. Nocera, D. Fukumura, R. K. Jain and M. G. Bawendi, *J. Am. Chem. Soc.*, 2010, **132**, 472.
16 E. Petryayeva and U. J. Krull, *Langmuir*, 2012, **28**, 13943.
17 A. B. Greytak, P. M. Allen, W. Liu, J. Zhao, E. R. Young, Z. Popović, B. J. Walker, D. G. Nocera and M. G. Bawendi, *Chem. Sci.*, 2012, **3**, 2028.
18 M. L. Hoarfrost and R. A. Segalman, *Macromolecules*, 2011, **44**, 5281.
19 E. Petryayeva, W. R. Algar and U. J. Krull, *Langmuir*, 2013, **29**, 977.
20 W. Wang, A. Kapur, X. Ji, M. Safi, G. Palui, V. Palomo, P. E. Dawson and H. Mattoussi, *J. Am. Chem. Soc.*, 2015, **137**, 5438.
21 K. E. Sapsford, T. Pons, I. L. Medintz, S. Higashiya, F. M. Brunel, P. E. Dawson and H. Mattoussi, *J. Phys. Chem. C*, 2007, **111**, 11528.
22 R. Shunmugam and G. N. Tew, *J. Polym. Sci., Part A: Polym. Chem.*, 2005, **43**, 5831.
23 L. K. Van Vugt, B. Piccione, C.-H. Cho, C. Aspetti, A. D. Wirshba and R. Agarwal, *J. Phys. Chem. A*, 2011, **115**, 3827.
24 M. H. Allen, S. T. Hemp, A. E. Smith and T. E. Long, *Macromolecules*, 2012, **45**, 3669.
25 C. Luo, Y. Liu and Z. Li, *Soft Matter*, 2012, **8**, 2618.
26 A. M. Alb, P. Enohnyaket, M. F. Drenski, R. Shunmugam, G. N. Tew and W. F. Reed, *Macromolecules*, 2006, **39**, 8283.
27 M. J. Yanjarappa, K. V. Gujraty, A. Joshi, A. Saraph and R. S. Kane, *Biomacromolecules*, 2006, **7**, 1665.

28 G. J. Reddy, S. V. Naidu and A. V. R. Reddy, *J. Appl. Polym. Sci.*, 2003, **90**, 2179.
29 C. Soykan, A. Delibaş and R. Coşkun, *React. Funct. Polym.*, 2008, **68**, 114.
30 M. Kucharski and R. Lubczak, *J. Appl. Polym. Sci.*, 1997, **64**, 1259.
31 A. Viswanath, Y. Shen, A. N. Green, R. Tan, A. B. Greytak and B. C. Benicewicz, *Macromolecules*, 2014, **47**, 8137.
32 A. Wamsley, B. Jasti, P. Phiasivongsa and X. Li, *J. Polym. Sci., Part A: Polym. Chem.*, 2004, **42**, 317.
33 P. Theato, *J. Polym. Sci., Part A: Polym. Chem.*, 2008, **46**, 6677.

This journal is © The Royal Society of Chemistry 2015